

Lewis Acid-Induced Change from Four- to Two-Electron Reduction of Dioxygen Catalyzed by Copper Complexes Using Scandium Triflate

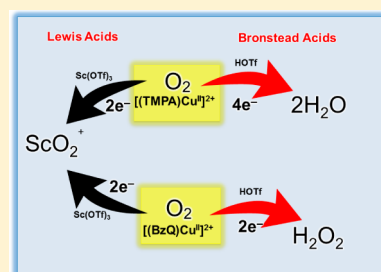
Saya Kakuda,^{†,§} Clarence J. Rolle,^{‡,§} Kei Ohkubo,[†] Maxime A. Siegler,[‡] Kenneth D. Karlin,^{*,‡} and Shunichi Fukuzumi^{*,†}

[†]Department of Material and Life Science, Division of Advanced Science and Biotechnology, Graduate School of Engineering, Osaka University, ALCA (JST), Suita, Osaka 565-0871, Japan

[‡]Department of Chemistry, Johns Hopkins University, Baltimore, Maryland 21218, United States

S Supporting Information

ABSTRACT: Mononuclear copper complexes, $[(\text{tmpa})\text{Cu}^{\text{II}}(\text{CH}_3\text{CN})](\text{ClO}_4)_2$ (**1**, tmpa = tris(2-pyridylmethyl)amine) and $[(\text{BzQ})\text{Cu}^{\text{II}}(\text{H}_2\text{O})_2](\text{ClO}_4)_2$ (**2**, BzQ = bis(2-quinolinylmethyl)benzylamine), act as efficient catalysts for the selective two-electron reduction of O_2 by ferrocene derivatives in the presence of scandium triflate ($\text{Sc}(\text{OTf})_3$) in acetone, whereas **1** catalyzes the four-electron reduction of O_2 by the same reductant in the presence of Brønsted acids such as triflic acid. Following formation of the peroxy-bridged dicopper(II) complex $[(\text{tmpa})\text{Cu}^{\text{II}}(\text{O}_2)\text{Cu}^{\text{II}}(\text{tmpa})]^{2+}$, the two-electron reduced product of O_2 with Sc^{3+} is observed to be scandium peroxide ($[\text{Sc}^{\text{III}}(\text{O}_2^{2-})]^+$). In the presence of 3 equiv of hexamethylphosphoric triamide (HMPA), $[\text{Sc}^{\text{III}}(\text{O}_2^{2-})]^+$ was oxidized by $[\text{Fe}(\text{bpy})_3]^{3+}$ (bpy = 2,2-bipyridine) to the known superoxide species $[(\text{HMPA})_3\text{Sc}^{\text{III}}(\text{O}_2^{\bullet-})]^{2+}$ as detected by EPR spectroscopy. A kinetic study revealed that the rate-determining step of the catalytic cycle for the two-electron reduction of O_2 with **1** is electron transfer from Fc^* to **1** to give a cuprous complex which is highly reactive toward O_2 , whereas the rate-determining step with **2** is changed to the reaction of the cuprous complex with O_2 following electron transfer from ferrocene derivatives to **2**. The explanation for the change in catalytic O_2 -reaction stoichiometry from four-electron with Brønsted acids to two-electron reduction in the presence of Sc^{3+} and also for the change in the rate-determining step is clarified based on a kinetics interrogation of the overall catalytic cycle as well as each step of the catalytic cycle with study of the observed effects of Sc^{3+} on copper–oxygen intermediates.



INTRODUCTION

Copper proteins play important roles in oxidation of substrates accompanied by two-electron reduction of dioxygen (O_2) to hydrogen peroxide (H_2O_2) or four-electron reduction of O_2 to water (H_2O) depending on the type of enzymes.¹ For example, in the oxidation of their substrates, galactose oxidases² and amine oxidases³ effect the two-electron reduction of O_2 to hydrogen peroxide,⁴ whereas multicopper oxidases (MCO's)⁵ and heme-copper oxidases (HCO's)⁶ facilitate the four-electron reduction of O_2 to H_2O . The catalytic four-electron reduction of O_2 with synthetic copper complexes as well as other metal complexes has merited special attention because of not only the mechanistic interest in relation to MCO's but also in development of a fuel cell technology and their application using earth-abundant metals such as iron, cobalt, and copper.^{7–15} On the other hand, the catalytic two-electron reduction of O_2 to H_2O_2 has also attracted increasing interest, because H_2O_2 is regarded as a promising candidate as a high-density energy carrier as compared with gaseous hydrogen and also H_2O_2 can be used as a liquid fuel in simple one-compartment fuel cells.^{16–18} There have been many reports on the electrocatalytic and homogeneous four-electron reduction of O_2 with copper complexes.^{16–24} In contrast, there has been only few examples for the catalytic two-electron reduction of O_2 using a copper complex.²⁵ Whether copper complexes are effective for two-

four-electron reduction of O_2 depends on a variety of factors, including the ligand type and resulting nature of copper–oxygen intermediates formed as reactive species in the O_2 reduction catalysis.^{24,25} The counteranions of proton sources employed also affect the O_2 -reduction catalytic reactivity with copper complexes, with-respect-to the observed stoichiometry and/or mechanism of reaction.^{24–26} However, there has been no report on the change in the number of electrons to reduce O_2 (two-electron vs four-electron) in O_2 reduction catalysis induced by metal ions acting as Lewis acids.

We report herein the drastic change to a two-electron from a four-electron reduction of O_2 with $[(\text{tmpa})\text{Cu}^{\text{II}}(\text{CH}_3\text{CN})](\text{ClO}_4)_2$ (**1**) induced by the Lewis acid $[\text{Sc}(\text{OTf})_3]$. In contrast to the case of **1**, the selective two-electron reduction of O_2 occurred with $[(\text{BzQ})\text{Cu}^{\text{II}}(\text{H}_2\text{O})_2](\text{ClO}_4)_2$ (**2**) in the presence of triflic acid (HOTf) as well as $\text{Sc}(\text{OTf})_3$. The mechanism of the selective two-electron reduction of O_2 with **1** and **2** is examined by a kinetics study of the overall catalytic cycle as well as each step of the catalytic cycle with study of the observed effects of Sc^{3+} on copper–oxygen intermediates.

Received: December 11, 2014

Published: February 7, 2015

EXPERIMENTAL SECTION

Materials. The following reagents were obtained commercially and used as received: Scandium triflate [$\text{Sc}(\text{OTf})_3$], decamethylferrocene (Fc^*), 1,1'-dimethylferrocene (Me_2Fc), ferrocene (Fc), triflic acid, hydrogen peroxide (30%), and NaI (Wako Pure Chemical Industries). Following literature procedures,²⁷ acetone was dried and distilled under Ar. The compounds $[(\text{tmpa})\text{Cu}^{\text{II}}(\text{CH}_3\text{CN})](\text{ClO}_4)_2$ (**1**)²⁸ and bis(2-quinolinylmethyl)benzylamine (BzQ)^{29,30} were prepared as described.

$[(\text{BzQ})\text{Cu}^{\text{II}}(\text{H}_2\text{O})_2](\text{ClO}_4)_2$ (**2**). A 50 mL flask was charged with BzQ (389 mg, 1.0 mmol) and $\text{Cu}(\text{ClO}_4)_2 \cdot 6\text{H}_2\text{O}$ (370 mg, 1.0 mmol). To this was added 20 mL MeOH. The solution became blue and with stirring after 1 h and yielded a precipitate consisting of blue microcrystals. The solid product **2** was collected employing a vacuum filtration procedure, then washed with 15 mL MeOH, and dried under vacuum. (599 mg, 0.86 mmol, 86% yield) Anal. calcd ($\text{C}_{28}\text{H}_{29}\text{Cl}_2\text{CuO}_{10}\text{N}_3$): C, 47.14; H, 3.96; N, 6.11. Found: C, 47.15; H, 3.87; N, 6.06. X-ray quality crystals were obtained by allowing pentane to slowly diffuse into a saturated acetone solution of **2**.

Single Crystal X-ray Crystallography. All reflection intensities were measured at 110(2) K using a SuperNova diffractometer (with Atlas detector) and Cu $K\alpha$ radiation ($\lambda = 1.54178 \text{ \AA}$) using the CrysAlisPro program (Version 1.171.36.32 Agilent Technologies, 2013); the latter was also employed to refine cell dimensions and for data reduction. The structure was solved and refined on F^2 using SHELXS-2013 (Sheldrick, 2013). Analytical numeric absorption corrections based on a multifaceted crystal model were applied using CrysAlisPro. The data collection temperature was controlled using a Cryojet (Oxford Instruments) system. Unless otherwise specified, the H atoms were placed at calculated positions using AFIX 23, AFIX 43, or AFIX 137 instructions with isotropic displacement parameters with values 1.2 or 1.5 times U_{eq} for the C atoms attached. The H atoms attached to O1W*n*, O2W*n*, and O3W*n* ($n = 1, 2$) (coordinated water molecules) were found from difference Fourier maps, and their coordinates were refined freely (DFIX instructions were used to restrain the O–H and H...H distances within acceptable ranges).

There are three crystallography independent Cu(II) complexes, six ClO_4^- perchlorate anions, plus seven lattice acetone solvate molecules per asymmetric unit. The structure is mostly ordered. Five of the six counterions are disordered over two orientations. The occupancy factors of the major components of the disorder refine to 0.871(6), 0.54(2), 0.661(6), 0.591(4), and 0.560(16).

$\text{C}_{102}\text{H}_{123}\text{Cl}_6\text{Cu}_3\text{N}_9\text{O}_{37}$. Moiety formula: $3(\text{C}_{27}\text{H}_{27}\text{CuN}_3\text{O}_2)$, $6(\text{ClO}_4)$, $7(\text{C}_3\text{H}_6\text{O})$, $F_w = 2470.41$, blue block, $0.34 \times 0.33 \times 0.18 \text{ mm}^3$, monoclinic, $P2_1/n$ (no. 14), $a = 22.8236(3)$, $b = 12.18146(19)$, $c = 39.6106(6) \text{ \AA}$, $\beta = 92.6704(13)^\circ$, $V = 11000.8(3) \text{ \AA}^3$, $Z = 4$, $D_x = 1.492 \text{ g cm}^{-3}$, $\mu = 2.760 \text{ mm}^{-1}$, $T_{\text{min}} - T_{\text{max}}$: 0.474–0.684. 73408 Reflections were measured up to a resolution of $(\sin \theta/\lambda)_{\text{max}} = 0.62 \text{ \AA}^{-1}$. 21523 Reflections were unique ($R_{\text{int}} = 0.0243$), of which 19284 were observed [$I > 2\sigma(I)$]. 1682 Parameters were refined using 746 restraints. $R1/wR2$ [$I > 2\sigma(I)$]: 0.0341/0.0914. $R1/wR2$ [all refl.]: 0.0388/0.0948. $S = 1.028$. Residual electron density found between -0.55 and 0.66 e \AA^{-3} . The molecular weight is given for the moiety formula.

Reaction Procedure. Spectral changes [Hewlett-Packard 8453 photodiode-array spectrophotometer with a quartz cuvette (path length = 10 mm)] at 298 K were observed as a function of varying $\text{Sc}(\text{OTf})_3$ concentrations during the dioxygen catalytic reduction experiments. Employing a microsyringe, an acetone solution of $\text{Sc}(\text{OTf})_3$ was added to an O_2 -saturated acetone solution containing $[(\text{tmpa})\text{Cu}^{\text{II}}(\text{CH}_3\text{CN})](\text{ClO}_4)_2$ (**1**) ($1.0 \times 10^{-5} \text{ M}$) or $[(\text{BzQ})\text{Cu}^{\text{II}}(\text{H}_2\text{O})_2](\text{ClO}_4)_2$ (**2**) ($1.0 \times 10^{-4} \text{ M}$) and Fc^* ($2.0 \times 10^{-3} \text{ M}$). Fc^{*+} and Me_2Fc^+ concentrations being produced during the reaction were determined from known absorptivity data, $\lambda_{\text{max}} = 780 \text{ nm}$ ($\epsilon = 500 \text{ M}^{-1} \text{ cm}^{-1}$ at 298 K and $600 \text{ M}^{-1} \text{ cm}^{-1}$ at 213 K) for $\text{Me}_2\text{Fc}^{*+}$ and $\lambda_{\text{max}} 650 \text{ nm}$, $\epsilon_{\text{max}} = 360 \text{ M}^{-1} \text{ cm}^{-1}$ for Me_2Fc^+ . For Fc^{*+} the extinction coefficient was estimated by carrying out a Fc^* electron-transfer oxidation using $[\text{Ru}^{\text{III}}(\text{bpy})_3](\text{PF}_6)_3$. The limiting concentration of O_2 in an acetone solution was prepared by a mixed gas flow of O_2 and N_2 , using a gas mixer (Kofloc GB-3C, KOJIMA Instrument Inc.) that was able to effect

controlled pressure and flow rate mixing of two gases. Hydrogen peroxide determination was carried out by standard iodide titration where the O_2 reduction product solution in acetone was diluted and reacted with NaI in excess. Quantitation of the I_3^- formed was then calculated using its visible spectrum ($\lambda_{\text{max}} = 361 \text{ nm}$, $\epsilon = 2.5 \times 10^4 \text{ M}^{-1} \text{ cm}^{-1}$).³¹ All low-temperature UV–vis absorption spectra and spectral changes were recorded using a Hewlett-Packard 8453A diode array spectrophotometer with attached liquid nitrogen cooled cryostat (Unisoku USP-203-A).

Kinetic Measurements. Fast reactions with short half-lives ($\leq 10 \text{ s}$) at 298 K were performed with a UNISOKU RSP-601 stopped flow spectrophotometer possessing a MOS-type high selective photodiode array and attached Unisoku thermostated cell holder. The kinetics of electron transfer from Fc^* to **1** were analyzed by monitoring absorption band changes due to Fc^{*+} formation. Pseudo-first-order conditions were used throughout, with Fc^* concentrations kept at more than a 10-fold excess compared to that of **1**.

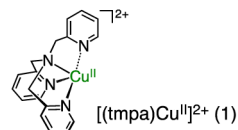
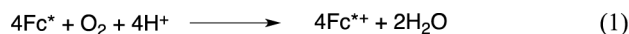
Electrochemistry. Copper(II) complex cyclic voltammetry using an ALS 630B electrochemical analyzer was utilized for measurements at 1 atm and under nitrogen or argon, both in the presence and absence of $\text{Sc}(\text{OTf})_3$; conditions included use of deaerated acetone solutions with 0.1 M $[(n\text{-butyl})_4\text{N}]\text{PF}_6$ (TBAPF_6) all at RT. A platinum working electrode (surface area of 0.3 mm^2) was employed within a conventional three-electrode cell using a Pt counter electrode. The BAS platinum working electrode was often polished with an alumina suspension (BAS); prior to use, acetone was used to wash the electrode. The reference electrode used was Ag/AgNO_3 (0.01 M), and to convert potentials to values vs the SCE, 0.29 V was added.³²

EPR Measurements. A JEOL JES-RE1XE spectrometer was used to record EPR spectra of Cu(II) and scandium superoxide complexes. The modulation amplitude employed was selected to optimize the signal-to-noise (S/N) ratio and resolution under conditions of non-saturating microwave power. A Mn^{2+} marker inserted into the EPR cavity was used to determine g values and hyperfine coupling constants.

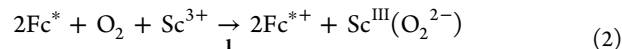
Theoretical Calculations. Using a 32-processor QuantumCube with Gaussian 09 (revision A.02), DFT calculations on copper complexes were performed. A UCAM-B3LYP/6-311G(d) level of theory was employed for geometry optimization.^{33–36} Computational results graphical output were generated using GaussView (ver. 3.09; Semichem, Inc.).³⁷

RESULTS AND DISCUSSION

Catalytic Two-Electron Reduction of O_2 by Fc^* with **1 in the Presence of $\text{Sc}(\text{OTf})_3$.** We have previously reported that $[(\text{tmpa})\text{Cu}^{\text{II}}(\text{CH}_3\text{CN})](\text{ClO}_4)_2$ (**1**) ($\text{tmpa} = \text{tris}(2\text{-pyridylmethyl})\text{amine}$) catalyzed the four-electron reduction of O_2 by decamethylferrocene (Fc^*) to H_2O in the presence of perchloric acid or trifluoroacetic acid in acetone as shown in eq 1: where 4 equiv of Fc^{*+} (decamethylferrocenium ion)



was formed.^{24a,26} When $\text{Sc}(\text{OTf})_3$ is employed as a Lewis acid instead of HClO_4 or CF_3COOH , **1** also efficiently catalyzes the reduction of O_2 where Fc^{*+} is also produced (Figure 1). In this case, however, the stoichiometry of O_2 reduction is different and follows eq 2:



where 2 equiv of Fc^{*+} ($\lambda_{\text{max}} = 780 \text{ nm}$) relative to O_2 is produced and 1 equiv of Sc^{3+} is consumed instead of four

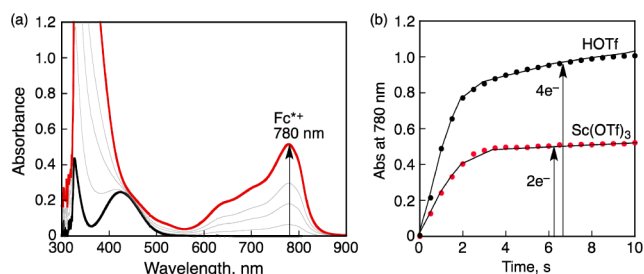


Figure 1. (a) UV-vis spectral changes observed in the two-electron and four-electron reduction of O_2 (0.5 mM) by Fc^* (2.0 mM) with $Sc(OTf)_3$ (2.0 mM) catalyzed by **1** (40 μM) in acetone at 298 K. (b) Time courses of absorbance at 780 nm due to Fc^{*+} in the two-electron and four-electron reduction of O_2 (0.5 mM) by Fc^* (2.0 mM) catalyzed by **1** (40 μM) in the presence of $Sc(OTf)_3$ (2.0 mM) and HOTf (40 mM), respectively.

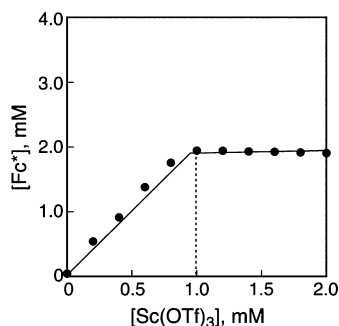
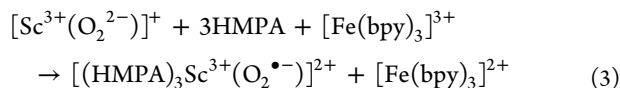


Figure 2. Plot of absorbance at 780 nm due to Fc^{*+} vs concentration of $Sc(OTf)_3$ in the two-electron reduction of O_2 (2.5 mM) by Fc^* (2.0 mM) with $Sc(OTf)_3$ (0–2.0 mM) catalyzed by **1** (40 μM) in acetone at 298 K.

protons (eq 1), as shown in the spectral titration in Figure 2. The reduced product of O_2 is $[Sc^{III}(O_2^{2-})]^+$, based on the stoichiometry determined (Figure 2). The yield of $[Sc^{III}(O_2^{2-})]^+$ was determined to be 100% based on an iodometric titration (Figure S1 in Supporting Information (SI)).³¹

To further support the formation of scandium peroxide ($[Sc^{III}(O_2^{2-})]^+$), the reaction mixture was oxidized using the one-electron oxidant ($[Fe(bpy)_3]^{3+}$), which was stabilized in the presence of 3 equiv of the hexamethylphosphoric triamide (HMPA) ligand to produce ($[(HMPA)_3Sc^{III}(O_2^{\bullet-})]^{2+}$), as shown by eq 3.³⁷ The formation of ($[(HMPA)_3Sc^{III}(O_2^{\bullet-})]^{2+}$



was detected by EPR spectroscopy as shown in Figure 3. The g value (2.0112) and superhyperfine coupling constant due to scandium ($I = 7/2$; $a(Sc) = 3.82$ G) are the same as those reported previously.³⁸ The end-on coordination of $O_2^{\bullet-}$ to Sc^{3+} is indicated by inequivalent $a(^{17}O)$ values (14 and 17 G)³⁸ and supported by optimized geometry calculations by an unrestricted Hartree–Fock (UHF) SCF optimization using the 6-311++G** basis set.³⁹ In contrast to the case for this superoxo complex, DFT calculations suggest that the side on structure of the peroxo complex ($[Sc^{III}(O_2^{2-})]^+$) is more stable than an end-on coordinated peroxo-scandium species (Figure S2 in SI).

Kinetics and Mechanism of Catalytic Two-Electron Reduction of O_2 by Fc^* with **1.** The rate of formation of

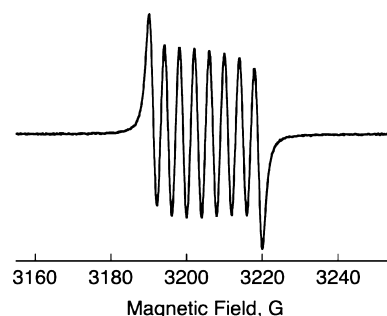


Figure 3. EPR spectrum observed after addition of $[Fe^{III}(bpy)_3]^{3+}$ and HMPA (30 mM) to an N_2 -saturated acetone solution of $[Sc^{III}(O_2^{2-})]^+$, which was produced by the two-electron reduction of O_2 (11 mM) by Fc^* in the presence of $[(tmpa)Cu^{II}](ClO_4)_2$ (**1**) (10 μM) and $Sc(OTf)_3$ (10 mM) in acetone at 298 K. The g value is 2.011, confirming the production of the known HMPA-Sc-superoxo complex.

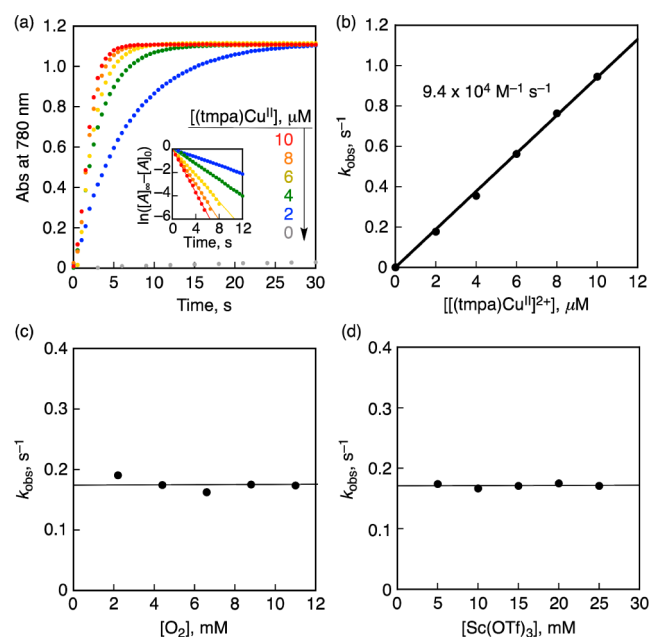


Figure 4. (a) Time profiles of formation of Fc^{*+} monitored by absorbance at 780 nm ($\epsilon = 500$ $M^{-1} cm^{-1}$) in the two-electron reduction of O_2 by Fc^* (2.0 mM) with $Sc(OTf)_3$ (10 mM) catalyzed by **1** (2–10 μM) in saturated ($[O_2] = 11$ mM) acetone at 298 K. Inset: First-order plots. (b) Plot of k_{obs} vs $[1]$ for the two-electron reduction of O_2 by Fc^* (2.0 mM) in the presence of $Sc(OTf)_3$ (10 mM) in acetone at 298 K. (c) Plot of k_{obs} vs $[O_2]$ for the two-electron reduction of O_2 by Fc^* (2.0 mM) catalyzed by **1** (2.0 μM) in saturated ($[O_2] = 11$ mM) acetone at 298 K. (d) Plot of k_{obs} vs $[Sc(OTf)_3]$ for the two-electron reduction of O_2 by Fc^* (2.0 mM) with $Sc(OTf)_3$ (5–25 mM) catalyzed by **1** (2 μM) in saturated ($[O_2] = 11$ mM) acetone at 298 K.

Fc^{*+} in the two-electron reduction of O_2 by Fc^* with **1** was monitored by an increase in absorbance at 780 nm due to Fc^{*+} . The rate obeyed pseudo-first-order kinetics in the presence of excess $Sc(OTf)_3$ and O_2 relative to Fc^* (Figure 4a). The observed pseudo-first-order rate constant (k_{obs}) increases linearly with increasing concentration of **1** (Figure 4b), whereas the k_{obs} value remained constant with increasing concentration of O_2 (Figure 4c). The k_{obs} value was also constant at the $Sc(OTf)_3$ concentration above 5 mM (Figure 4d). Thus, the kinetic formulation of the two-electron reduction of O_2 by

Fc^* with **1** in the presence of large excess $\text{Sc}(\text{OTf})_3$ is given by eq 4:

$$d[\text{Fc}^{*+}]/dt = k_{\text{cat}}[\mathbf{1}][\text{Fc}^*] \quad (4)$$

where k_{cat} is the second-order catalytic rate constant of **1**. The k_{cat} value was determined to be $(9.4 \pm 0.5) \times 10^4 \text{ M}^{-1} \text{ s}^{-1}$ at 298 K. This value is twice of the rate constant (k_{et}) of electron transfer from Fc^* to **1** ($5.0 \pm 0.1) \times 10^5 \text{ M}^{-1} \text{ s}^{-1}$ in acetone at 298 K,^{24a} i.e., $k_{\text{cat}} = 2k_{\text{et}}$ because the electron transfer should occur twice to reduce O_2 in the catalytic cycle when two equiv of Fc^{*+} is formed. This indicates that electron transfer from Fc^* to **1** is the rate-determining step in the catalytic two-electron reduction of O_2 by Fc^* with **1**. In such a case, **1** should remain as the cupric complex $[(\text{tmpa})\text{Cu}^{\text{II}}]^{2+}$ during the catalytic two-electron reduction reaction. This was confirmed by the observation of the EPR spectrum of **1** as measured during catalysis as shown in Figure 5, where the EPR spectrum

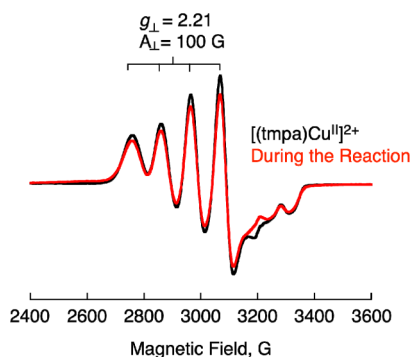


Figure 5. EPR spectra of $[(\text{tmpa})\text{Cu}^{\text{II}}]^{2+} **1** (0.10 mM) (black line) measured at 77 K during the catalytic two-electron reduction of O_2 (11 mM) by Fc^* (2 mM) with $\text{Sc}(\text{OTf})_3$ (10 mM) at 298 K (red line). EPR parameters of $[(\text{tmpa})\text{Cu}^{\text{II}}]^{2+}$: $g_{\perp} = 2.21$, $|A_{\perp}| = 100 \text{ G}$, $g_{\parallel} = 2.00$, $|A_{\parallel}| = 64 \text{ G}$.$

(red line) during the reaction is the same as $[(\text{tmpa})\text{Cu}^{\text{II}}]^{2+}$ before the reaction (black line).

Electron transfer from Fc^* to **1** is followed by the well-established nearly diffusion controlled binding of O_2 to $[(\text{tmpa})\text{Cu}^{\text{I}}]^+$ producing superoxo complex ($[(\text{tmpa})\text{Cu}^{\text{II}}(\text{O}_2)]^+$) that further rapidly reacts with $[(\text{tmpa})\text{Cu}^{\text{I}}]^+$ to afford the peroxy complex (*trans*- μ -1,2-peroxy-dicopper complex ($[(\text{tmpa})\text{Cu}^{\text{II}}(\text{O}_2)\text{Cu}^{\text{II}}(\text{tmpa})]^{2+}$) (Figure 6), where the absorption band at 520 nm due to the peroxy complex was observed by the reaction of $[(\text{tmpa})\text{Cu}^{\text{I}}]^+$ with O_2 at 213 K.^{24a,26} The addition of 1 equiv of $\text{Sc}(\text{OTf})_3$ (2 mM) to an acetone solution of the peroxy complex resulted in disappearance of the absorption band due to the peroxy complex, accompanied by appearance of the absorption band at 394 nm, which is tentatively assigned to the Sc^{3+} -bound peroxy complex, $[(\text{tmpa})\text{Cu}^{\text{II}}(\text{O}_2)\text{Sc}(\text{OTf})_3]^+$; the conversion exhibits an isosbestic point (Figure 6a,b). At prolonged reaction times, absorption bands at both 394 and 520 nm decayed to yield $[(\text{tmpa})\text{Cu}^{\text{II}}]^{2+}$ (blue line in Figure 6c) and $[\text{Sc}^{\text{III}}(\text{O}_2^{2-})]^+$.

Based on the results described above, the catalytic cycle of the two-electron reduction of O_2 by Fc^* with **1** in the presence of $\text{Sc}(\text{OTf})_3$ is proposed as shown in Scheme 1. Electron transfer from Fc^* to **1** is the rate-determining step to produce Fc^{*+} and $[(\text{tmpa})\text{Cu}^{\text{I}}]^+$, which rapidly reacts with O_2 to produce the superoxo complex ($[(\text{tmpa})\text{Cu}^{\text{II}}(\text{O}_2)]^+$). There are two pathways of the further reaction of $[(\text{tmpa})\text{Cu}^{\text{II}}(\text{O}_2)]^+$.

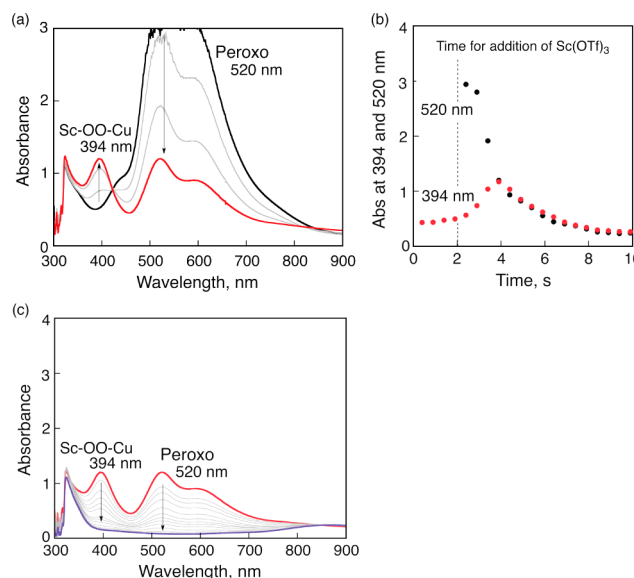
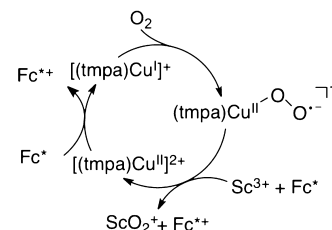


Figure 6. (a,c) UV-vis absorption spectral change in the reaction of $[(\text{tmpa})\text{Cu}^{\text{I}}]^+$ (2.0 mM) with O_2 in O_2 -saturated acetone (black), followed by addition of $\text{Sc}(\text{OTf})_3$ (2.0 mM) to the resulting solution at 213 K (red) at (a) 0–4 s and (c) 4–10 s time delays. (b) Absorption time profiles at 394 nm due to the Sc^{3+} -bound peroxy complex, $[(\text{tmpa})\text{Cu}^{\text{II}}(\text{O}_2)\text{Sc}(\text{OTf})_3]^+$ and 520 nm due to $[(\text{tmpa})\text{Cu}^{\text{II}}(\text{O}_2)\text{Cu}^{\text{II}}(\text{tmpa})]^{2+}$. $\text{Sc}(\text{OTf})_3$ was added at a 2 s time delay.

Scheme 1



One is the reaction of $[(\text{tmpa})\text{Cu}^{\text{II}}(\text{O}_2)]^+$ with $[(\text{tmpa})\text{Cu}^{\text{I}}]^+$ to produce the peroxy complex ($[(\text{tmpa})\text{Cu}^{\text{II}}(\text{O}_2)\text{Cu}^{\text{II}}(\text{tmpa})]^{2+}$) which reacts with Sc^{3+} to yield $[(\text{tmpa})\text{Cu}^{\text{II}}]^{2+}$ and $[\text{Sc}^{\text{III}}(\text{O}_2^{2-})]^+$ (Figure 6). In such a case, the catalytic rate constant would be the same as the rate constant of electron transfer from Fc^* to $[(\text{tmpa})\text{Cu}^{\text{II}}]^{2+}$ ($k_{\text{cat}} = k_{\text{et}}$). Because $k_{\text{cat}} = 2k_{\text{et}}$ (vide supra), the superoxo complex ($[(\text{tmpa})\text{Cu}^{\text{II}}(\text{O}_2)]^+$) may be rapidly reduced by Fc^* with Sc^{3+} to produce Fc^{*+} and $[\text{Sc}^{\text{III}}(\text{O}_2^{2-})]^+$, accompanied by regeneration of $[(\text{tmpa})\text{Cu}^{\text{II}}]^{2+}$ (Scheme 1).

When $\text{Sc}(\text{OTf})_3$ was replaced by trivalent metal triflates such as $\text{Yb}(\text{OTf})_3$, $\text{Y}(\text{OTf})_3$ and $\text{Lu}(\text{OTf})_3$, which are weaker Lewis acid than $\text{Sc}(\text{OTf})_3$,^{38–40} the catalytic reactivity of the two-electron reduction of O_2 by Fc^* with **1** becomes lower than that of $\text{Sc}(\text{OTf})_3$ as shown in Figure 7. Divalent metal triflates such as $\text{Mg}(\text{OTf})_2$ and $\text{Ca}(\text{OTf})_2$, which are still weaker Lewis acid than trivalent metal triflates,^{39–42} exhibited lower reactivity, and the reaction was stopped before completion (Figure 7). Thus, strong Lewis acidity of metal ions is required for the efficient catalytic two-electron reduction of O_2 by Fc^* with **1**.

When Fc^* was replaced by a weaker one-electron reductant such as 1,1'-dimethylferrocene (Me_2Fc), no electron transfer from Me_2Fc ($E_{\text{ox}} = 0.28 \text{ V vs SCE}$) to **1** ($E_{\text{red}} = -0.05 \text{ V vs SCE}$) occurred, leading to no catalytic reduction of O_2 in the

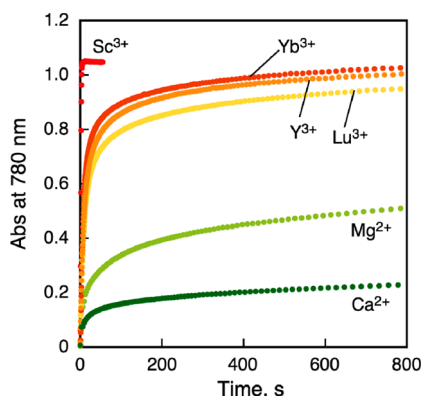


Figure 7. Time courses of absorbance at 780 nm due to Fc^{3+} in the two-electron reduction of O_2 (11 mM) by Fc^* (2.0 mM) with metal triflates [$\text{Sc}(\text{OTf})_3$, $\text{Yb}(\text{OTf})_3$, $\text{Y}(\text{OTf})_3$, $\text{Lu}(\text{OTf})_3$, $\text{Mg}(\text{OTf})_2$, and $\text{Ca}(\text{OTf})_2$] (2.0 mM) catalyzed by **1** (40 μM) in acetone at 298 K.

presence of $\text{Sc}(\text{OTf})_3$. Thus, we examined the catalytic reduction of O_2 by Me_2Fc in the presence of $\text{Sc}(\text{OTf})_3$ using a copper(II) complex which has a more positive E_{red} value than **1** (vide infra).

Catalytic Two-Electron Reduction of O_2 by Me_2Fc with **2 in the Presence of $\text{Sc}(\text{OTf})_3$.** Pyridyl ligand alterations which introduce steric effects are known to result in a decrease in the donor ability to a Cu(II) center, which causes a positive shift in the redox potential of Cu(II) complexes.³⁰ In order to use milder reductants for the reduction of dioxygen, we synthesized $[(\text{BzQ})\text{Cu}^{\text{II}}(\text{H}_2\text{O})_2](\text{ClO}_4)_2$ (**2**) as a potential catalyst. Complex **2** was generated by the addition of BzQ to $\text{Cu}(\text{ClO}_4)_2 \cdot 6\text{H}_2\text{O}$ in MeOH and characterized by elemental analysis. Recrystallization of **2** from acetone/pentane afforded crystals suitable for X-ray structure determination; the structure of **2** is shown in Figure 8.⁴³ The steric effect of quinoline ligand is recognized as the elongated Cu–N bonds as compared with those of $[(\text{tmpa})\text{Cu}^{\text{II}}]^{2+}$.

The E_{red} value of **2** was determined to be 0.44 V vs SCE, which is much more positive than that of **1** (–0.05 V vs SCE),

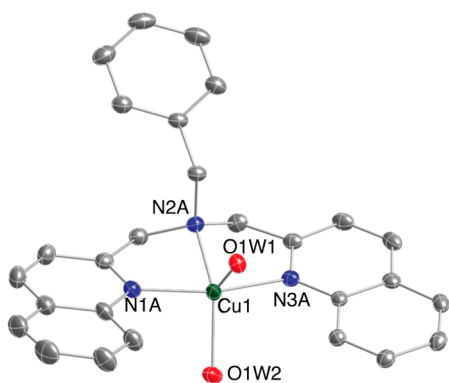
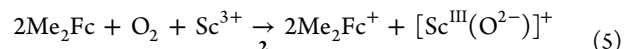


Figure 8. Displacement ellipsoid plot (50% probability level) of one crystallographically independent cation of $[\text{Cu}^{\text{II}}(\text{BzQ})(\text{H}_2\text{O})_2](\text{ClO}_4)_2 \cdot 2.33(\text{C}_3\text{H}_6\text{O})$ ($\text{BzQ})\text{Cu}^{\text{II}}$; the two remaining cations, the ClO_4^- counteranions, and the lattice acetone solvent molecules have been omitted for clarity. Selected bond distances: Cu1–N1A, 1.9950(14) Å; Cu1–N2A, 2.0494(14) Å; Cu1–N3, 1.9958(14) Å; Cu1–O1W1, 2.1934(12) Å; Cu1–O1W2, 2.0002(13). Selected bond angles: N1A–Cu1–N3A, 165.60(6)°; N1A–Cu1–N2A, 83.21(6)°; N2A–Cu1–N3A, 83.82.39(6)°; N1A–Cu1–O1W1, 90.69(5)°; O1W1–Cu1–O1W2, 108.97(5)°; N2A–Cu1–O1W2, 141.95(6)°.

thus the two-electron reduction of O_2 by Me_2Fc became possible using **2** as a catalyst in the presence of $\text{Sc}(\text{OTf})_3$ in acetone at 298 K (eq 5). The stoichiometry is the same as in



eq 2, where 1 equiv of Sc^{3+} was consumed for formation of 2 equiv of Me_2Fc^+ (Figure S3 in SI). Ferrocene itself can also be used to reduce O_2 to $[\text{Sc}^{\text{III}}(\text{O}_2^{2-})]^+$ with **2** and $\text{Sc}(\text{OTf})_3$, although the rate is slower than that of Me_2Fc because of the higher E_{ox} value of Fc (0.37 V vs SCE) than that of Me_2Fc ($E_{\text{ox}} = 0.28$ V vs SCE).

The rate of formation of Me_2Fc^+ obeyed pseudo-zero-order kinetics as shown in Figure 9a, where the initial rate of

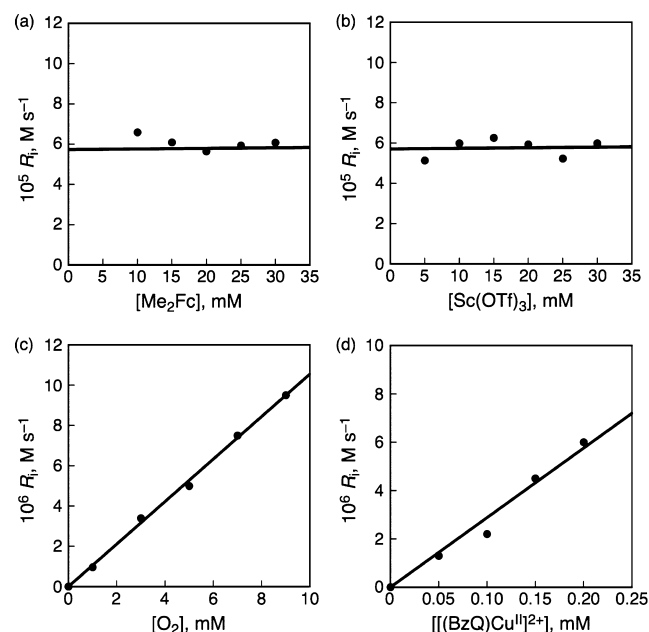


Figure 9. (a) Plot of the initial rate of formation of Me_2Fc^+ vs $[\text{Me}_2\text{Fc}]$ in the two-electron reduction of O_2 by Me_2Fc with $\text{Sc}(\text{OTf})_3$ (10 mM) catalyzed by **2** (0.2 mM) in saturated ($[\text{O}_2] = 11$ mM) acetone at 298 K. (b) Plot of the initial rate of formation of Me_2Fc^+ vs $[\text{Sc}(\text{OTf})_3]$ in the two-electron reduction of O_2 by Me_2Fc (10 mM) with $\text{Sc}(\text{OTf})_3$ catalyzed by **2** (0.20 mM) in saturated ($[\text{O}_2] = 11$ mM) acetone at 298 K. (c) Plot of k_{obs} vs $[\text{O}_2]$ for the two-electron reduction of O_2 by Me_2Fc (10 mM) with $\text{Sc}(\text{OTf})_3$ (10 mM) catalyzed by **2** (0.2 mM) in acetone at 298 K. (d) Plot of k_{obs} vs $[\mathbf{2}]$ for the two-electron reduction of O_2 by Me_2Fc (10 mM) with $\text{Sc}(\text{OTf})_3$ (10 mM) catalyzed by **2** in saturated ($[\text{O}_2] = 11$ mM) acetone at 298 K.

formation of Me_2Fc^+ (R_i) is independent of concentration of Me_2Fc . R_i is also independent of concentration of Sc^{3+} (Figure 9b), whereas R_i is proportional to concentrations of O_2 and **2** as shown in Figure 9c,d, respectively. Thus, the rate of formation of the two-electron reduction of O_2 by Me_2Fc with **2** in the presence of large excess $\text{Sc}(\text{OTf})_3$ is given by eq 6:

$$d[\text{Me}_2\text{Fc}^+]/dt = k_{\text{cat}}'[\text{O}_2][\mathbf{2}] \quad (6)$$

where k_{cat}' is the second-order catalytic rate constant.

Because the catalytic rate is proportional to concentrations of O_2 and **2**, but independent of concentrations of Me_2Fc or Sc^{3+} , the rate-determining step in the catalytic cycle is the reaction of $[(\text{BzQ})\text{Cu}^{\text{I}}]^+$ with O_2 . In such a case, **2** is converted to $[(\text{BzQ})\text{Cu}^{\text{I}}]^+$ during the catalytic two-electron reduction of O_2 by Me_2Fc with **2**. This was confirmed by disappearance of

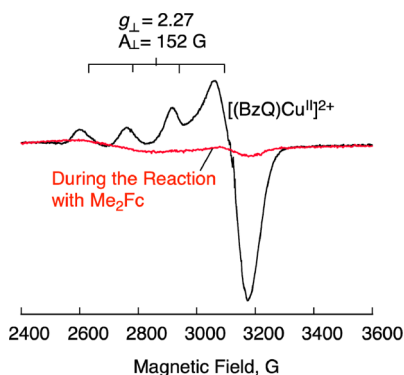


Figure 10. EPR spectra of $[(\text{BzQ})\text{Cu}^{\text{II}}]^{2+}$ (**2**) (0.10 mM) (black line) observed at 77 K, $[(\text{BzQ})\text{Cu}^{\text{I}}]^+$ (0.05 mM) produced during the catalytic reduction of oxygen (2.2 mM) in the presence of Me_2Fc (10 mM) and $\text{Sc}(\text{OTf})_3$ (10 mM) (red line).

EPR spectrum of **2** measured during the catalysis as shown in Figure 10, where the EPR signal due to **2** (black line) is converted to the Cu^{I} complex, which is EPR silent (red line).

The reaction of the Cu^{I} complex of **2** with O_2 was previously reported to afford copper(II)–oxygen intermediates different than that known for the case of **1**, that are a $(\eta^2:\eta^2\text{-peroxo})\text{-dicopper(II)}$ complex ($\lambda_{\text{max}} = 362$ and 535 nm) plus a bis($\mu\text{-oxo}$)dicopper(III) species ($\lambda_{\text{max}} = 394$ nm) (see Figure 11a,

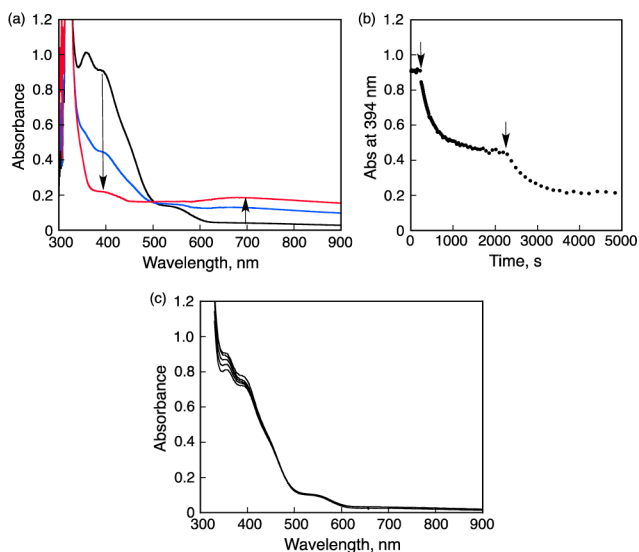
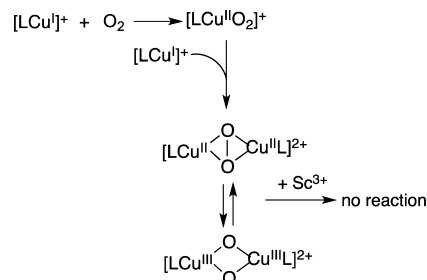


Figure 11. (a) UV–vis spectral changes observed upon the addition of 2 eq of HOTf (4.0 mM) to the mixture of the $\mu\text{-}\eta^2\text{-}\eta^2\text{-}(\text{side-on})$ peroxo dinuclear copper(II) complex and the bis- $\mu\text{-oxo}$ dinuclear copper(III) complex. (b) Absorption time profiles at 394 nm due to the addition of HOTf (4.0 mM) to the mixture of the $\mu\text{-}\eta^2\text{-}\eta^2\text{-}(\text{side-on})$ peroxo dinuclear copper(II) complex and the bis- $\mu\text{-oxo}$ dinuclear copper(III) complex. (c) UV–vis spectral changes observed upon the addition of $\text{Sc}(\text{OTf})_3$ (4.0 mM) to the mixture of the $\mu\text{-}\eta^2\text{-}\eta^2\text{-}(\text{side-on})$ peroxo dinuclear copper(II) complex and the bis- $\mu\text{-oxo}$ dinuclear copper(III) complex.

black line); the mixture had been characterized by resonance Raman spectroscopy.³⁰ The addition of 2 equiv HOTf to an acetone solution of the peroxo and bis- $\mu\text{-oxo}$ complexes resulted in the decomposition of the $\text{Cu}\text{-O}_2$ species to release H_2O_2 (Figure 11b). In contrast, the addition of $\text{Sc}(\text{OTf})_3$ to an acetone solution of the peroxo and bis- $\mu\text{-oxo}$ complexes

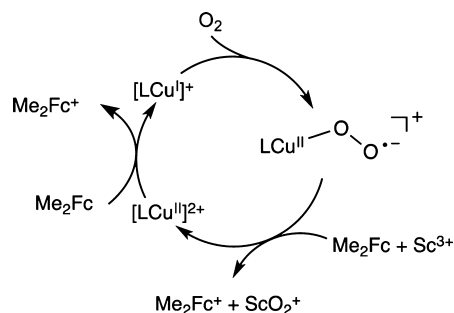
Scheme 2



resulted in little change in absorption bands of the $\text{Cu}\text{-O}_2$ intermediates (Figure 11c), indicating that these complexes are stable against Sc^{3+} (Scheme 2).

Thus, once the $\mu\text{-}\eta^2\text{-}\eta^2\text{-}(\text{side-on})$ peroxo dinuclear copper(II) complex and the bis- $\mu\text{-oxo}$ dinuclear copper(III) complex are formed via the superoxo complex, no catalytic reduction of O_2 by Me_2Fc would occur with **2** in the presence of $\text{Sc}(\text{OTf})_3$. Under the catalytic conditions, the superoxo complex is reduced by Me_2Fc in the presence of Sc^{3+} to yield Me_2Fc^+ and $\text{Sc}(\text{O}_2)^+$, accompanied by regeneration of **2** without formation of the $\mu\text{-}\eta^2\text{-}\eta^2\text{-}(\text{side-on})$ peroxo dinuclear copper(II) complex or the bis- $\mu\text{-oxo}$ dinuclear copper(III) complex as shown in Scheme 3. The rate-determining step in Scheme 3 is

Scheme 3



the reaction of $[(\text{BzQ})\text{Cu}^{\text{I}}]^+$ with O_2 to produce the superoxo complex, when the catalytic rate is proportional to concentrations of O_2 and **2**, but independent of concentrations of Me_2Fc or Sc^{3+} as observed in Figure 9.

CONCLUSION

The four-electron reduction of O_2 by Fc^* with a mononuclear complex $[(\text{tpma})\text{Cu}^{\text{I}}(\text{CH}_3\text{CN})](\text{ClO}_4)_2$ (**1**) in the presence of a proton source (HOTf) was changed to the two-electron reduction of O_2 by replacing Brønsted acids by $\text{Sc}(\text{OTf})_3$ that acts as a strong Lewis acid. The rate-determining step of the catalytic cycle is found to be electron transfer from Fc^* to O_2 . When **1** was replaced by a copper(II) complex $[(\text{BzQ})\text{Cu}^{\text{II}}(\text{H}_2\text{O})_2](\text{ClO}_4)_2$ (**2**), which has a more positive reduction potential as compared with **1**, the catalytic two-electron reduction of O_2 is made possible by using a weaker one-electron reductant than Fc^* such as Me_2Fc and Fc . In this case, the rate-determining step is the reaction of $[(\text{BzQ})\text{Cu}^{\text{I}}]^+$ with O_2 to produce the superoxo complex. The Lewis acid-induced change in the stoichiometry of the catalytic O_2 reduction provides a new way to control this important biological or chemical “fuel-cell” reaction which can produce either hydrogen peroxide or water.

■ ASSOCIATED CONTENT

■ Supporting Information

Spectral and kinetic analytical data, theoretical calculation data (Figures S1–S6), and X-ray crystallographic data (pdf); crystallographic file (cif). This material is available free of charge via the Internet at <http://pubs.acs.org>.

■ AUTHOR INFORMATION

Corresponding Authors

*fukuzumi@chem.eng.osaka-u.ac.jp

*karlin@jhu.edu

Author Contributions

[§]These authors contributed equally.

Notes

The authors declare no competing financial interest.

■ ACKNOWLEDGMENTS

This work was supported by an Advanced Low Carbon Technology Research and Development (ALCA) program from Japan Science Technology Agency (JST) to S.F., the Japan Society for the Promotion of Science (JSPS: Grants 20108010 to S.F. and 26620154 and 26288037 to K.O.) sponsored by the MEXT (Japan), and by KOSEF/MEST through the WCU Project (R31-2008-000-10010-0). K.D.K. also acknowledges support from the USA National Institutes of Health.

■ REFERENCES

- (1) (a) Solomon, E. I.; Heppner, D. E.; Johnston, E. M.; Ginsbach, J. W.; Cirera, J.; Qayyum, M.; Kieber-Emmons, M. T.; Kjaergaard, C. H.; Hadt, R. G.; Tian, L. *Chem. Rev.* **2014**, *114*, 3659. (b) Kosman, D. J. *J. Biol. Inorg. Chem.* **2010**, *15*, 15. (c) Battaini, G.; Granata, A.; Monzani, E.; Gullotti, M.; Casella, L. *Adv. Inorg. Chem.* **2006**, *58*, 185. (d) Rosenzweig, A. C. *Nat. Chem.* **2009**, *1*, 684.
- (2) Humphreys, K. J.; Mirica, L. M.; Wang, Y.; Klinman, J. P. *J. Am. Chem. Soc.* **2009**, *131*, 4657–4663.
- (3) Mukherjee, A.; Smirnov, V. V.; Lanci, M. P.; Brown, D. E.; Shepard, E. M.; Dooley, D. M.; Roth, J. P. *J. Am. Chem. Soc.* **2008**, *130*, 9459–9473.
- (4) McGuirl, M. A.; Dooley, D. M. Copper Proteins with Type 2 Sites. In *Encyclopedia of Inorganic Chemistry*, 2nd ed.; King, R. B., Ed.; John Wiley & Sons Ltd.: Chichester, 2005; Vol. II, pp 1201–1225.
- (5) (a) Blanford, C. F.; Heath, R. S.; Armstrong, F. A. *Chem. Commun.* **2007**, 1710. (b) Mano, N.; Soukharev, V.; Heller, A. *J. Phys. Chem. B* **2006**, *110*, 11180–11187.
- (6) (a) Pereira, M. M.; Santana, M.; Teixeira, M. *Biochim. Biophys. Acta* **2001**, *1505*, 185. (b) Winter, M.; Brodd, R. J. *Chem. Rev.* **2004**, *104*, 4245. (c) Ferguson-Miller, S.; Babcock, G. T. *Chem. Rev.* **1996**, *96*, 2889. (d) Hosler, J. P.; Ferguson-Miller, S.; Mills, D. A. *Annu. Rev. Biochem.* **2006**, *75*, 165. (e) Kaila, V. R. I.; Verkhovskiy, M. I.; Wikström, M. *Chem. Rev.* **2010**, *110*, 7062.
- (7) (a) Fukuzumi, S.; Karlin, K. D. *Coord. Chem. Rev.* **2013**, *257*, 187. (b) Fukuzumi, S. *Chem. Lett.* **2008**, *37*, 808.
- (8) (a) Collman, J. P.; Devaraj, N. K.; Decréau, R. A.; Yang, Y.; Yan, Y.-L.; Ebina, W.; Eberspacher, T. A.; Chidsey, C. E. D. *Science* **2007**, *315*, 1565. (b) Collman, J. P.; Decréau, R. A.; Lin, H.; Hosseini, A.; Yang, Y.; Dey, A.; Eberspacher, T. A. *Proc. Natl. Acad. Sci. U.S.A.* **2009**, *106*, 7320. (c) Collman, J. P.; Ghosh, S.; Dey, A.; Decréau, R. A.; Yang, Y. *J. Am. Chem. Soc.* **2009**, *131*, 5034.
- (9) (a) Rosenthal, J.; Nocera, D. G. *Acc. Chem. Res.* **2007**, *40*, 543. (b) Chang, C. J.; Loh, Z.-H.; Shi, C.; Anson, F. C.; Nocera, D. G. *J. Am. Chem. Soc.* **2004**, *126*, 10013. (c) Dogutan, D. K.; Stoian, S. A.; McGuire, R.; Schwalbe, M.; Teets, T. S.; Nocera, D. G. *J. Am. Chem. Soc.* **2011**, *133*, 131. (d) Teets, T. S.; Cook, T. R.; McCarthy, B. D.; Nocera, D. G. *J. Am. Chem. Soc.* **2011**, *133*, 8114.
- (10) (a) Halime, Z.; Kotani, H.; Li, Y.; Fukuzumi, S.; Karlin, K. D. *Proc. Natl. Acad. Sci. U.S.A.* **2011**, *108*, 13990. (b) Fukuzumi, S.; Okamoto, K.; Gros, C. P.; Guillard, R. *J. Am. Chem. Soc.* **2004**, *126*, 10441. (c) Fukuzumi, S.; Okamoto, K.; Tokuda, Y.; Gros, C. P.; Guillard, R. *J. Am. Chem. Soc.* **2004**, *126*, 17059. (d) Fukuzumi, S.; Mandal, S.; Mase, M.; Ohkubo, K.; Park, H.; Benet-Buchholz, J.; Nam, W.; Llobet, A. *J. Am. Chem. Soc.* **2012**, *134*, 9906.
- (11) (a) Fukuzumi, S.; Mochizuki, S.; Tanaka, T. *Inorg. Chem.* **1989**, *28*, 2459. (b) Fukuzumi, S.; Mochizuki, S.; Tanaka, T. *Inorg. Chem.* **1990**, *29*, 653. (c) Fukuzumi, S.; Mochizuki, S.; Tanaka, T. *J. Chem. Soc., Chem. Commun.* **1989**, 391.
- (12) Vielstich, W.; Lamm, A.; Gasteiger, H. A. *Handbook of fuel cells: fundamentals, technology, and applications*; Wiley: Chichester, U.K., 2003.
- (13) (a) Zagal, J. H.; Griveau, S.; Silva, J. F.; Nyokong, T.; Bedioui, F. *Coord. Chem. Rev.* **2010**, *254*, 2755. (b) Li, W.; Yu, A.; Higgins, D. C.; Llanos, B. G.; Chen, Z. *J. Am. Chem. Soc.* **2010**, *132*, 17056.
- (14) (a) Gewirth, A. A.; Thorum, M. S. *Inorg. Chem.* **2010**, *49*, 3557. (b) Stambouli, A. B.; Traversa, E. *Renew. Sust. Energy Rev.* **2002**, *6*, 295. (c) Marković, N. M.; Schmidt, T. J.; Stamenković, V.; Ross, P. N. *Fuel Cells* **2001**, *1*, 105. (d) Steele, B. C. H.; Heinzl, A. *Nature* **2001**, *414*, 345.
- (15) Asahi, M.; Yamazaki, S.-i.; Itoh, S.; Ioroi, T. *Dalton Trans.* **2014**, 43, 10705.
- (16) (a) Honda, T.; Kojima, T.; Fukuzumi, S. *J. Am. Chem. Soc.* **2012**, *134*, 4196. (b) Mase, K.; Ohkubo, K.; Fukuzumi, S. *J. Am. Chem. Soc.* **2013**, *135*, 2800.
- (17) (a) Disselkamp, R. S. *Energy Fuels* **2008**, *22*, 2771. (b) Disselkamp, R. S. *Int. J. Hydrogen Energy* **2010**, *35*, 1049.
- (18) (a) Fukuzumi, S.; Yamada, Y.; Karlin, K. D. *Electrochim. Acta* **2012**, *82*, 493. (b) Yamada, Y.; Fukunishi, Y.; Yamazaki, S.; Fukuzumi, S. *Chem. Commun.* **2010**, 46, 7334. (c) Yamada, Y.; Yoshida, S.; Honda, T.; Fukuzumi, S. *Energy Environ. Sci.* **2011**, *4*, 2822. (d) Shaegh, S. A. M.; Nguyen, N.-T.; Ehteshami, S. M. M.; Chan, S. H. *Energy Environ. Sci.* **2012**, *5*, 8225.
- (19) (a) Zhang, J.; Anson, F. C. *J. Electroanal. Chem.* **1992**, *341*, 323. (b) Zhang, J.; Anson, F. C. *J. Electroanal. Chem.* **1993**, *348*, 81. (c) Zhang, J.; Anson, F. C. *Electrochim. Acta* **1993**, *38*, 2423. (d) Lei, Y.; Anson, F. C. *Inorg. Chem.* **1994**, *33*, 5003.
- (20) (a) Weng, Y. C.; Fan, F.-R. F.; Bard, A. J. *J. Am. Chem. Soc.* **2005**, *127*, 17576. (b) Thorum, M. S.; Yadav, J.; Gewirth, A. A. *Angew. Chem., Int. Ed.* **2009**, *48*, 165.
- (21) (a) McCrory, C. C. L.; Ottenwaelder, X.; Stack, T. D. P.; Chidsey, C. E. D. *J. Phys. Chem. A* **2007**, *111*, 12641. (b) McCrory, C. C. L.; Devadoss, A.; Ottenwaelder, X.; Lowe, R. D.; Stack, T. D. P.; Chidsey, C. E. D. *J. Am. Chem. Soc.* **2011**, *133*, 3696.
- (22) (a) Pichon, C.; Mialane, P.; Dolbecq, A.; Marrot, J.; Riviere, E.; Keita, B.; Nadjio, L.; Secheresse, F. *Inorg. Chem.* **2007**, *46*, 5292. (b) Dias, V. L. N.; Fernandes, E. N.; da Silva, L. M. S.; Marques, E. P.; Zhang, J.; Marques, A. L. B. *J. Power Sources* **2005**, *142*, 10. (c) Losada, J.; del Peso, I.; Beyer, L. *Inorg. Chim. Acta* **2001**, *321*, 107.
- (23) (a) Thorseth, M. A.; Tornow, C. E.; Tse, E. C. M.; Gewirth, A. A. *Coord. Chem. Rev.* **2013**, *257*, 130. (b) Thorseth, M. A.; Letko, C. S.; Rauchfuss, T. B.; Gewirth, A. A. *Inorg. Chem.* **2011**, *50*, 6158.
- (24) (a) Fukuzumi, S.; Kotani, H.; Lucas, H. R.; Doi, K.; Suenobu, T.; Peterson, R. L.; Karlin, K. D. *J. Am. Chem. Soc.* **2010**, *132*, 6874. (b) Fukuzumi, S.; Tahsini, L.; Lee, Y.-M.; Ohkubo, K.; Nam, W.; Karlin, K. D. *J. Am. Chem. Soc.* **2012**, *134*, 7025. (c) Tahsini, L.; Kotani, H.; Lee, Y.-M.; Cho, J.; Nam, W.; Karlin, K. D.; Fukuzumi, S. *Chem.–Eur. J.* **2012**, *18*, 1084. (d) Das, D.; Lee, Y.-M.; Ohkubo, K.; Nam, W.; Karlin, K. D.; Fukuzumi, S. *J. Am. Chem. Soc.* **2013**, *135*, 4018.
- (25) Das, D.; Lee, Y.-M.; Ohkubo, K.; Nam, W.; Karlin, K. D.; Fukuzumi, S. *J. Am. Chem. Soc.* **2013**, *135*, 2825.
- (26) Kakuda, S.; Peterson, R. L.; Ohkubo, K.; Karlin, K. D.; Fukuzumi, S. *J. Am. Chem. Soc.* **2013**, *135*, 2825.
- (27) Armarego, W. L. F.; Chai, C. L. L. *Purification of Laboratory Chemicals*, 5th ed.; Butterworth-Heinemann: Oxford, 2003.

- (28) Wang, J.; Schopfer, M. P.; Puiu, S. C.; Sarjeant, A. A. N.; Karlin, K. D. *Inorg. Chem.* **2010**, *49*, 1404.
- (29) Kryatov, S. V.; Taktak, S.; Korendovych, I. V.; Rybak-Akimova, E. V.; Kaizer, J.; Torelli, S.; Shan, X.; Mandal, S.; MacMurdo, V.; Mairata i Payeras, A.; Que, L., Jr. *Inorg. Chem.* **2005**, *44*, 85.
- (30) Kunishita, A.; Osako, T.; Tachi, Y.; Teraoka, J.; Itoh, S. *Bull. Chem. Soc. Jpn.* **2006**, *79*, 1729.
- (31) (a) Mair, R. D.; Graupner, A. J. *J. Anal. Chem.* **1964**, *36*, 194. (b) Fukuzumi, S.; Kuroda, S.; Tanaka, T. *J. Am. Chem. Soc.* **1985**, *107*, 3020.
- (32) Mann, C. K.; Barnes, K. K. *Electrochemical Reactions in Nonaqueous Systems*; Marel Dekker: New York, 1990.
- (33) (a) Becke, A. D. *J. Chem. Phys.* **1993**, *98*, 5648. (b) Lee, C.; Yang, W.; Parr, R. G. *Phys. Rev. B* **1988**, *37*, 785.
- (34) (a) Hay, P. J.; Wadt, W. R. *J. Chem. Phys.* **1985**, *82*, 270. (b) Curtiss, L. A.; McGrath, M. P.; Blaudeau, J.-P.; Davis, N. E.; Binning, R. C., Jr.; Radom, L. *J. Chem. Phys.* **1995**, *103*, 6104.
- (35) (a) Yanai, T.; Tew, D. P.; Handy, N. C. *Chem. Phys. Lett.* **2004**, *393*, 51. (b) Tawada, Y.; Tsuneda, T.; Yanagisawa, S.; Yanai, T.; Hirao, K. *J. Chem. Phys.* **2004**, *120*, 8425.
- (36) Takaichi, J.; Ohkubo, K.; Sugimoto, H.; Nakano, M.; Usa, D.; Maekawa, H.; Fujieda, N.; Nishiwaki, N.; Seki, S.; Fukuzumi, S.; Itoh, S. *Dalton Trans.* **2013**, *42*, 2438.
- (37) Dennington, R., II; Keith, T.; Millam, J.; Eppinnett, K.; Hovell, W. L.; Gilliland, R. *Gaussview*; Semichem, Inc.: Shawnee Mission, KS, 2003.
- (38) (a) Fukuzumi, S.; Patz, M.; Suenobu, T.; Kuwahara, Y.; Itoh, S. *J. Am. Chem. Soc.* **1999**, *121*, 1605. (b) Kawashima, T.; Ohkubo, K.; Fukuzumi, S. *Phys. Chem. Chem. Phys.* **2011**, *13*, 3344.
- (39) (a) Fukuzumi, S.; Ohkubo, K. *Chem.–Eur. J.* **2000**, *6*, 4532. (b) Fukuzumi, S.; Ohkubo, K. *J. Am. Chem. Soc.* **2002**, *124*, 10270.
- (40) (a) Fukuzumi, S. *Prog. Inorg. Chem.* **2009**, *56*, 49. (b) Fukuzumi, S.; Ohkubo, K.; Morimoto, Y. *Phys. Chem. Chem. Phys.* **2012**, *14*, 8472.
- (41) Morimoto, Y.; Kotani, H.; Park, J.; Lee, Y.-M.; Nam, W.; Fukuzumi, S. *J. Am. Chem. Soc.* **2011**, *133*, 403.
- (42) When a weak Lewis acid, $\text{Mg}(\text{OTf})_2$ was applied to the catalyst for the O_2 reduction reaction with Fc^* , the absorption changes for formation of Fc^{*+} were significantly smaller as compared with the case of $\text{Sc}(\text{OTf})_3$ as shown in Figure 7.
- (43) The crystal structure of a similar copper(II) complex of BzQ-type ligand have already been reported. Osako, T.; Nagatomo, S.; Kitagawa, T.; Cramer, C. J.; Itoh, S. *J. Biol. Inorg. Chem.* **2005**, *10*, 581.